Raman and Photoluminescence Spectra for Ho, Er, Tm, Yb, Lu, and Y doped Hafnia

© *S.N. Shkerin*[1], *A.N. Meshcherskikh*[1], *T.V. Yaroslavtseva*[2], *R.K. Abdurakhimova*[1]

[1] Institute of High-Temperature Electrochemistry, Ural Branch, Russian Academy of Sciences,
Yekaterinburg, Russia
[2] Institute of Solid State Chemistry, Russian Academy of Sciences, Ural Branch,
Yekaterinburg, Russia

E-mail: shkerin@mail.ru

Previously obtained and certified HfO2 based samples were investigated by two Raman spectrometers with different wave source. Stokes reflexes have to be independent of the laser frequency so they were distinguished by comparison of different laser results. For the first time the dependence of Stokes lines frequencies on the cation radii of dopants was observed. Frequencies monotonically varied with the ratio of cation-dopant to hafnium radii changes. All non-Stokes reflexes are considered as photoluminescence. They were compared with both the literature data on luminescence of REM cations and the experimental results on zirconia-based materials intrinsic photoluminescence, which was a property of its point defects. Intrinsic photoluminescence is observed for the first time on hafnia-based materials.

Keywords: Raman spectroscopy, luminescence, hafnia with cubic structure, REE.

1. Introduction

Oxide materials with a fluorite structure — cerium, thorium, uranium dioxides, solid solutions based on them, as well as solid solutions based on zirconium and hafnium dioxides — have a defective lattice with an oxygen deficiency [1]. At the moment, the most studied are solid solutions based on zirconium dioxide doped with cations of lower valence, and are widely used as a solid oxygen-ion electrolyte for high-temperature electrochemical devices [1–10]. Prediction of the properties of such electrolytes requires understanding of their defect structure and, especially, the interaction of point defects with each other. Such interaction creates features of the behavior of the near-surface layer of materials [11–13], grain boundaries [14,15], conductivity [16–18], including its stability over time [19–21], thermal conductivity anomalies at low temperatures temperatures [22,23].

There are not so many methods of near-order research, and some of them are not readily available [24]. The most common method for studying the local structure is vibrational spectroscopy. However, Raman light scattering spectra, which for materials with a face-centered cubic (FCC) structure of the fluorite type usually give one band with T_{2g}-symmetry [25], in the case of materials based on zirconium dioxide show a significantly more complex picture. An example of such complex spectra

obtained for single crystal samples is presented, for example, in [26]. An analysis of light scattering mechanisms [27] shows that Stokes bands can be separated from other effects by means of monochromatic source with a different wavelength, because only linear Stokes effects are independent from wavelength of superimposed perturbation. In the study [28], two different monochromatic light sources with wavelengths of 532 and 785 nm were used, which made it possible to reliably isolate Stokes reflexes and study the near order in materials based on zirconium dioxide. In this study, two different monochromatic light sources are also used.

From the results of [28], it is obvious that the study of Raman scattering spectra for oxide materials with a FCC structure is greatly hampered by the presence of a large number of non-Stokes lines, this is due to luminescence. There can be singled out several causes of luminescence in these materials. The first one is associated with its own defective structure [29–33], which makes materials of this structural type unique. The observed effects have low intensity and increased sensitivity to experimental conditions [34], and, according to it-seems that due-to this they have been poorly known. The second — luminescence of f-elements (rare earth metals, REM) used as a dopant in these materials [35–46].

Solid solutions with a FCC-structure based on hafnium dioxide have been studied significantly weaker than similar materials based on zirconium dioxide [47]. It-seems this is
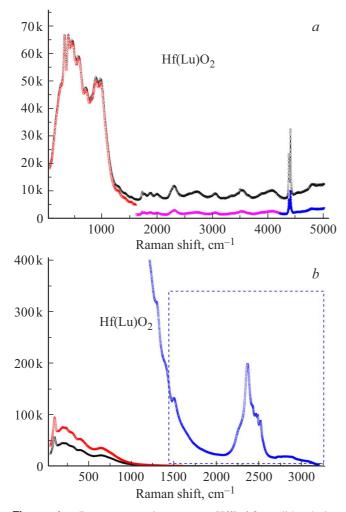
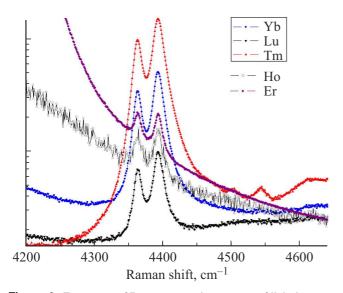**Figure 1.** Raman scattering spectra Hf(Lu)O$_2$ solid solution received in *a*) green and *b*) red radiation.

Figure 2. Fragments of Raman scattering spectra of light in green radiation.
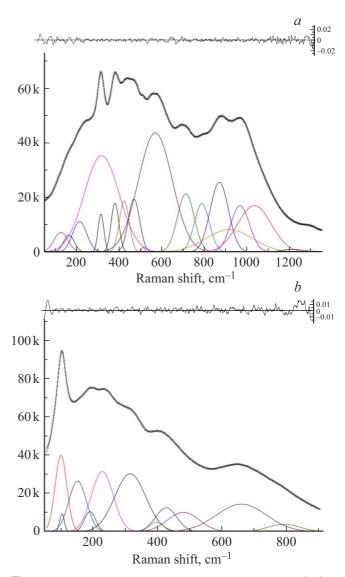

Figure 3. Decomposition of Raman scattering spectra Hf(Lu)O$_2$ solid solution received in *a*) green and *b*) red radiation by a set of Gaussian reflexes. The error of the description of the experimental data (points) of the fitting curve is shown at the top.

due to the fact that the electrical conductivity of [48–50] and the rate of electrode processes [51,52] is lower than that of similar solutions based on zirconium dioxide, despite higher stability under reducing conditions. Comparison of optical characteristics also showed similarity between zirconium and hafnium dioxides [53].

When studying ceramic samples of hafnium oxide doped with Lu, Yb, Tm, Er, Ho and Y sources with different wavelengths, it was possible to identify Stokes bands in the Raman scattering spectra. Comparison of photoluminescence spectra of materials based on hafnium dioxide with various doping and zirconium dioxide makes it possible to obtain luminescence of the defective structure of these materials.

Table 1. Results of analysis of the chemical composition of commercial hafnium dioxide by emission-spectral analysis with inductively coupled plasma („$<$***" means „below the specified detection limit ***")

Defined by parameter	Result analysis, mass%.	Defined by parameter	Result analysis, mass%
Ag_2O	<0.0005	Na_2O	1.483
Al_2O_3	6.0	Nb_2O_3	< 0.0004
As_2O_3	< 0.004	Nd_2O_3	< 0.002
AuO	< 0.0005	NiO	< 0.01
B_2O_3	< 0.002	P_2O_5	< 0.04
BaO	0.0148	PbO	< 0.01
BeO	< 0.00001	Pd	< 0.001
Bi_2O_3	< 0.006	Pr_2O_3	< 0.0008
CO_2	< 0.5	Pt	< 0.001
CaO	0.09	ReO_4	< 0.04
CdO	< 0.00002	Rh	< 0.0005
CeO_2	0.011	Ru	< 0.001
CoO	< 0.0002	SO_3	0.24
Cr_2O_3	0.0155	Sb_2O_3	< 0.003
CuO	< 0.0003	Sc_2O_3	3.66
Dy_2O_3	< 0.00008	Se_2O_3	< 0.007
< 0.0002	< 0.0002	SiO_2	11.478
< 0.00005	< 0.00005	Sm_2O_3	< 0.0008
Fe_2O_3	0.337	SnO_2	< 0.002
Ga_2O_3	< 0.005	SrO	0.002
Gd_2O_3	< 0.0002	Ta_2O_5	< 0.04
HfO_2	73.0088	Tb_2O_3	< 0.0002
Hg	< 0.0009	Te_2O_3	< 0.002
Ho_2O_3	< 0.0003	ThO_2	< 0.0003
IO_4	< 0.04	TiO_2	0.051
In_2O_3	< 0.002	Tl_2O_3	< 0.01
Ir	< 0.002	Tm_2O_3	< 0.001
K_2O	0.473	U_3O_8	< 0.002
La_2O_3	< 0.0004	V_2O_5	0.002
Li_2O	0.004	WO_3	< 0.01
Lu_2O_3	< 0.0003	Y_2O_3	0.7845
MgO	0.348	Yb_2O_3	0.002
MnO	0.013	ZnO	0.021
MoO_3	< 0.0009	ZrO_2	1.8518

2. Experimental procedure

Obtaining and certifying samples are described in detail in [50]. Synthesis of $Hf_{0.78}R_{0.22}O_{1.89}$ ($Hf(R)O_2$; $R =$ Y, Ho, Er, Tm, Yb, Lu) was carried out on a multi-stage solid-phase technology. As the initial reagents they used HfO_2 (class „os. h."), Er_2O_3 (99.99%), Lu_2O_3 (99.99%), Tm_2O_3 (99.99%), Yb_2O_3 (99.99%), Y_2O_3 (99.993%), Ho_2O_3 (99.99%). X-ray and SEM-studies have shown that the samples are single-phase, having a FCC-structure of the fluorite type, the lattice parameter of which monotonically increases with an increase in the ionic radius of the doping cation from lutetium to yttrium [50]. The chemical composition of hafnium dioxide was determined by emission spectral analysis with inductively coupled plasma on an Optima 4300 DV device manufactured by PerkinElmer (USA). The results of the certification are presented in Table 1.

Studies by Raman scattering method were performed using two different instruments:

– green radiation ($\lambda = 532$ nm) using a Renishaw U 1000 microscope-spectrometer. The laser power Nd : YAG was 50 mW;

Table 2. The luminescence wavelengths of the cations themselves, nm. Literature data — [58]

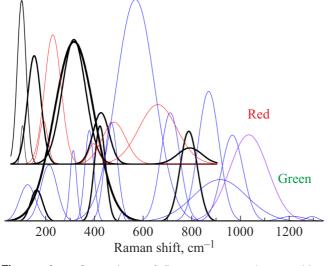| Lu	Yb		Tm		Er		Ho	
Exp.	Lit.	Exp.	Lit.	Exp.	Lit.	Exp.	Lit.	Exp.
545−555			−	*? [67,68]	533−534	540−550	543−548	536−554
						555−565		
					661	647−656		
			672−701	Very weak		Wide 647−684	651	Wide 634−668
			779−808	790−800		795−805	762	791−800
								Wide 798−837
					808	812−822		
						Wide 825−874	909	
965−975	975−1000	Triplet near970	−	965−975	975−987	969−979	−	968−978
						Wide 856−1034		Wide 924−1013

Figure 4. Comparison of Raman spectra decompositions Hf(Lu)O$_2$ solid solution obtained in green and red radiation. Bold black lines highlight Stokes bands that do not depend on the wavelength of the radiation used. Thin lines represent the bands caused by luminescence.
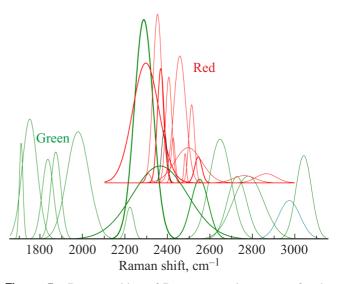

Figure 5. Decomposition of Raman scattering spectra for the solid solution Hf(Lu)O$_2$, in the area of large wave numbers.
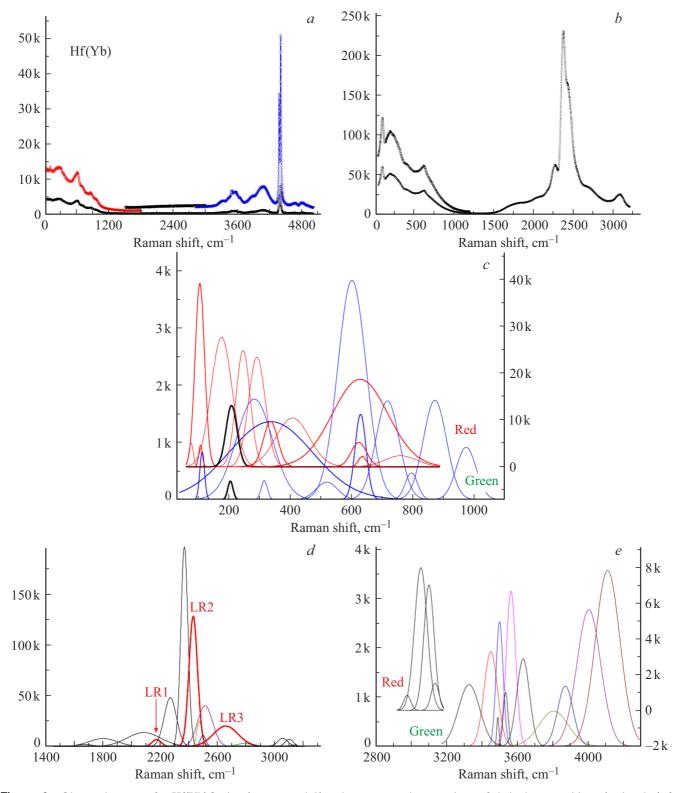
Figure 6. Observed spectra for Hf(Yb)O$_2$ in *a*) green and *b*) red sources, and comparison of their decompositions (*c*, *d* and *e*) for different parts of the spectrum. *d*) The bands LR1−LR3 are identified, identically coinciding with the luminescence spectrum of the ytterbium cation in the zirconium dioxide matrix [35].

– red radiation ($\lambda = 785$ nm) using InVia Reflex with a Leica DM2700 microscope. Power of the Renishaw diode laser with an integrated plasma filter was 300 mW.

Spectrum accumulation time is from 10 to 30 s, number of passes is from 5 to 16.

3. Results

Fig. 1 shows the Raman scattering spectra for the solid solution Hf(Lu)O$_2$, obtained in green (Fig. 1, a) and red (Fig. 1, b) radiation. Several curves are presented, differing in the time of accumulation of the spectrum and the number of passes, which allows you to highlight the features of its profile more contrastingly.

When using green radiation, a multiplet of narrow lines is detected, which do not depend on the nature of the doping cation (Fig. 2). No features of the spectra were detected when using control samples; thus, the lines observed in Fig. 2 are a reflection of the properties of the FCC proper-lattice of hafnium dioxide.

As can be seen from Fig. 1, and already noted earlier, for materials based on zirconium dioxide [28], the spectra have a complex profile that depends on the radiation used. Since only Stokes reflexes do not depend on the wavelength of the excitation used, the observed spectra were decomposed into a set of Gaussian-shaped lines (Fig. 3), and then compared with each other (Fig. 4). A similar approach was described in detail earlier [28]. Thus, the presence of four Stokes reflexes for Hf(Lu)O$_2$ (Fig. 4) was observed. All other lines reflect luminescence. Fig. 5 shows the decomposition of spectra in the area of large wave numbers reflecting the manifestation of luminescence. Comparison of the obtained and the literature data is difficult, due to the fact that the literature data on luminescence are presented depending either on the wavelength or on the energy of the quanta. The results of the recalculation in these coordinates will be presented below.

Fig. 6−10 shows the primary material for solid solutions of ytterbium, thulium, erbium, holmium and yttrium and the results of comparison of decompositions performed according to the method described in detail above for the sample Hf(Lu)O$_2$.

4. Discussion

4.1. Stokes lines

The optical properties of materials based on hafnium dioxide have not been studied in particular detail [54,55] as; this is due to the expectation that in general they are similar to the properties of materials based on zirconium dioxide [53]. Thus, luminescence and, in part, Raman spectroscopy of the above-mentioned solid solutions based on hafnium dioxide having a FCC-lattice have been studied for the first time. As has been shown for materials
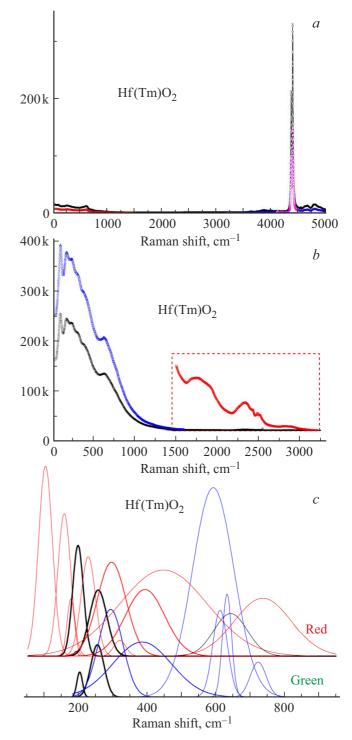

Figure 7. Observed spectra for Hf(Tm)O$_2$ in a) green and b) red sources, c) comparison of their decompositions.

based on zirconium dioxide [28], the study of Raman scattering spectra in these materials is significantly difficult. True Stokes reflexes do not depend on the wavelength of the disturbing source [27]. However, for these materials, they are disguised by additional reflexes, which are a manifestation of luminescence. Comparisons of reflexes
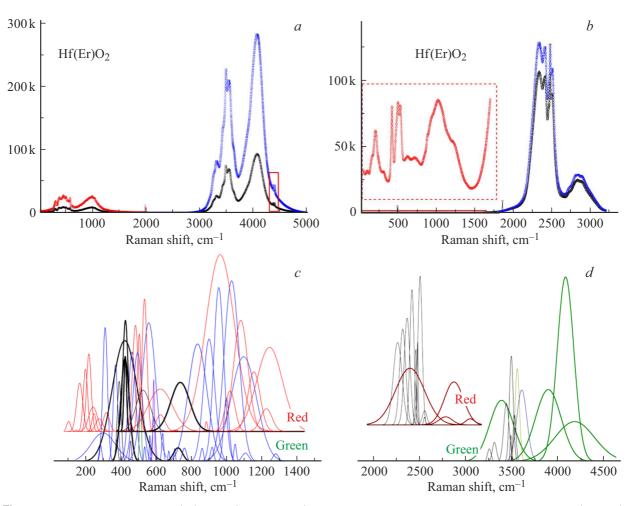
Figure 8. Observed spectra for Hf(Er)O_2 in *a*) green and *b*) red sources, and comparison of their decompositions (*c* and *d*).

obtained using red and green radiation sources are shown in Fig. 4 and 6, *c*−10, it c. The reflexes highlighted in these drawings with black bold lines do not depend on the wavelength of the radiation used. The frequencies of their manifestation are shown in Fig. 11, depending on the ratio of the radii of the doping cation to the radius of the hafnium cation in an octahedral environment.

According to the data of X-ray phase analysis, the structure of the materials is FCC of the fluorite type. For it, only one line [25] should be observed in the Raman spectra of light scattering. In full agreement with the previously obtained results for a material based on zirconium dioxide, we observe a number of lines that can be interpreted as a manifestation of a pyrochlore-type structure [35]. This structure is — related to the FCC-structure of the fluorite type and is the result of the interaction of defects with a change in the symmetry of the near environment.

The results of Fig. 11 can be interpreted in such a way that the wave numbers at which the corresponding bands appear decrease with an increase in the radius of the doping cation, in accordance with the ideas that the lattice strength should decrease with an increase in voltage. We note that

the contribution of luminescence is significant for erbium and holmium cations, therefore reliable isolation of Stokes reflexes in some areas of wave numbers is complicated.

4.2. Luminescence

All lines in Fig. 4 and 6, *c*−10, *c* is the result of luminescence manifestation. For the convenience of comparing our results with the literature data, we rearranged them depending on the wavelength of the recorded radiation (Fig. 12) — Stokes lines are excluded from consideration.

The most expected source of luminescence is transitions involving the energy levels of *f*- of REM electrons. Such spectra were studied when cations were placed in the crystal matrices of calcium fluorides [56] and lanthanum [57], as well as in aqueous solutions [58]. For oxide matrices, solutions of cations in the matrix of yttrium oxide [59–62] or lutetium [63–65] are most often studied. A particularly convenient object is the ytterbium cation, since it is characterized by only one line [56–58]. Study of ytterbium luminescence in a single crystal matrix KBaGd$(MoO_4)_3$, and a detailed overview of its manifestation in oxide matrices is given in [66]. The luminescence of the ytterbium
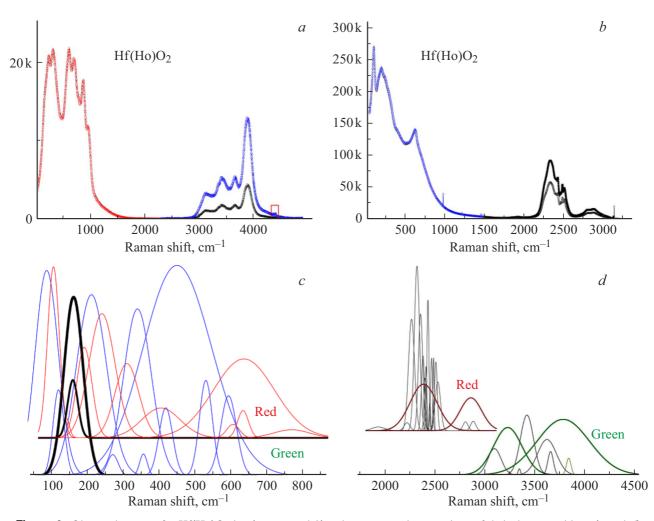
Figure 9. Observed spectra for Hf(Ho)O_2 in a) green and b) red sources, and comparison of their decompositions (c and d).

cation in a zirconium dioxide matrix was also studied in [35,37].

For materials based on zirconium dioxide, it was shown that in addition to luminescence due to REM cations, there is also luminescence due to intrinsic defects of the material [29–35]. It has a lower intensity than the luminescence of REM-cations, but its existence is beyond doubt. In this regard, in the obtained results, a band with a wavelength of about 690 nm attracts special attention (Fig. 2); it is common to all the samples studied, regardless of the nature of the doping cation. Impurity analysis (Table 1) did not allow the pollution to be isolated, which could be the cause of these reflexes. We note that the intensity of this band is much lower than the intensity of the bands reliably caused by the luminescence of cations (Ho and Er in Fig. 2). Suppose that these reflexes are an intrinsic property of defects in doped hafnium dioxide. They are observed for the first time. To exclude the nature of the impurity in our reagent (Table. 2) the Raman scattering spectra of light in single crystals based on hafnium dioxide used in the study [51] were investigated as the causes of these lines. They are obtained from especially pure raw materials in FIAN. There are also lines similar to those shown in Fig. 2. This indicates that these reflexes are an intrinsic property of defects in doped hafnium dioxide. They are observed for the first time.

Comparison (Fig. 1 for a green laser) of the intensity of bands in small wave numbers (near 550 nm in Fig. 12) and bands at 690 nm allows us to expect that luminescence in the area of 550 nm is present for lutetium. In addition, luminescence is assumed to be near 970 nm (Fig. 12), which we will consider in more detail below.

Unlike lutetium, only one band near 970 nm is actually observed for the ytterbium cation (Fig. 12). The observed triplet (highlighted in red in Fig. 12 and Fig. 6, d) absolutely coincides with the triplet shown for Zr(Yb)O_2 [35]. We note that there is also a set of lines, which we will consider in more detail below.

For thulium, the intrinsic luminescence of the cation in the area of excitation by a green laser was not detected (Fig. 7, a), but it can be assumed in the area of small wave numbers when excited by a red laser (Fig. 7, b). This is confirmed in independent papers [67,68].
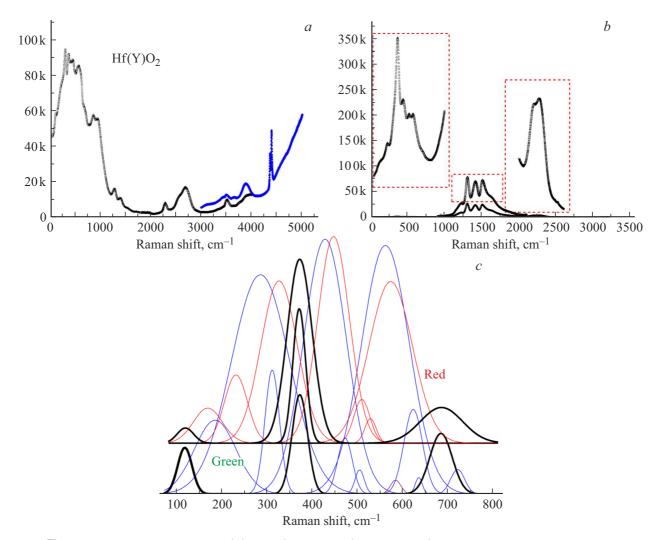
Figure 10. Observed spectra for Hf(Y)O$_2$ in *a*) green and *b*) red sources; *c*) comparison of their decompositions.
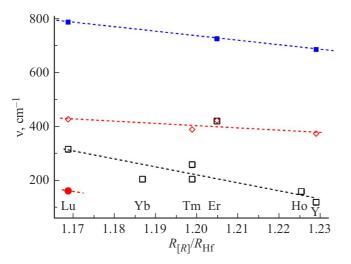

Figure 11. Dependence of the wave numbers of reflexes independent of the wavelength of the exciting radiation, based on the results of Figs. 4 and 6, *c*−10, *c* depending on the ratio of the radii of the doping cation to the radius of the hafnium cation in an octahedral environment.

For erbium and holmium, the high band intensities (Figs. 8 and 9) do not raise doubts about the significant contribution of luminescence. Part of the bands (Fig. 12) co-incides well with those described in the literature [69,70,37]. We note that the luminescence lines form multiplets that differ significantly in half-width. The wavelengths of the manifestation of reflexes, which we attributed to the contribution of the luminescence of the cations themselves, are summarized in Table 2.

For erbium and holmium cations (Table. 2 and Figs. 8 and 9) wide bands are observed, which is characteristic of luminescence as a result of transitions from centers characterized by a long lifetime. These lines are absent in studies in fluorides [56,57]. They are longer-wavelength (low-energy) satellites of standard narrow lines present both in our measurements and in the cited works. It-seems that they seem to reflect the interaction between the energy levels of REM and the energy levels of the oxide itself. A similar result is observed for these materials for the first time.
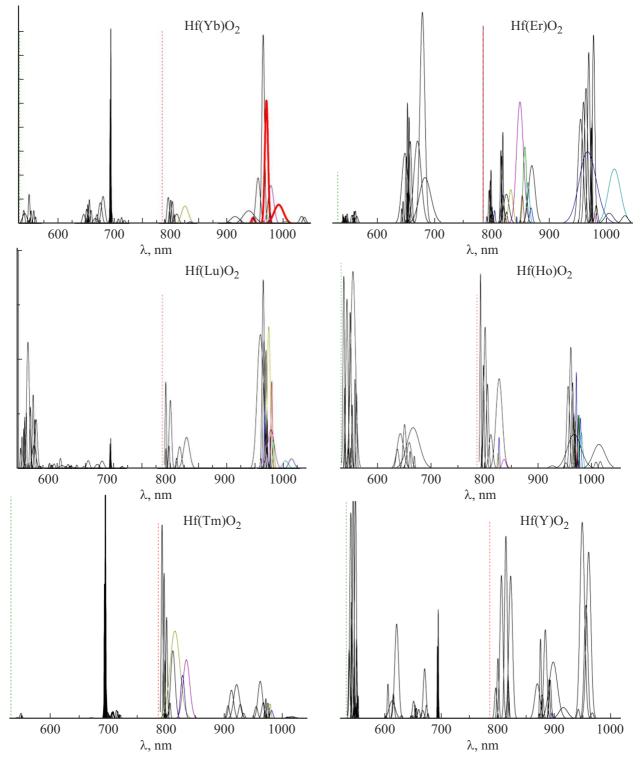
Figure 12. Observed luminescence lines in solid solutions based on hafnium dioxide. Vertical dotted lines highlight the wavelengths of exciting radiation. The intensities are not comparable with each other, since each group was divided based on the processing of a part of the spectra taken separately.

For hafnium oxide doped with yttrium (Fig. 10), no luminescence bands due to the doping cation can be observed. However, a set of luminescence lines is present (Fig. 12). The most interesting of them are — bands near 550 nm. Such reflexes are observed for pure yttrium oxide [59], which has a cubic structure C- of the rare earths type. In the study [62], these lines are discussed as a manifestation of certain point defects. It is interesting
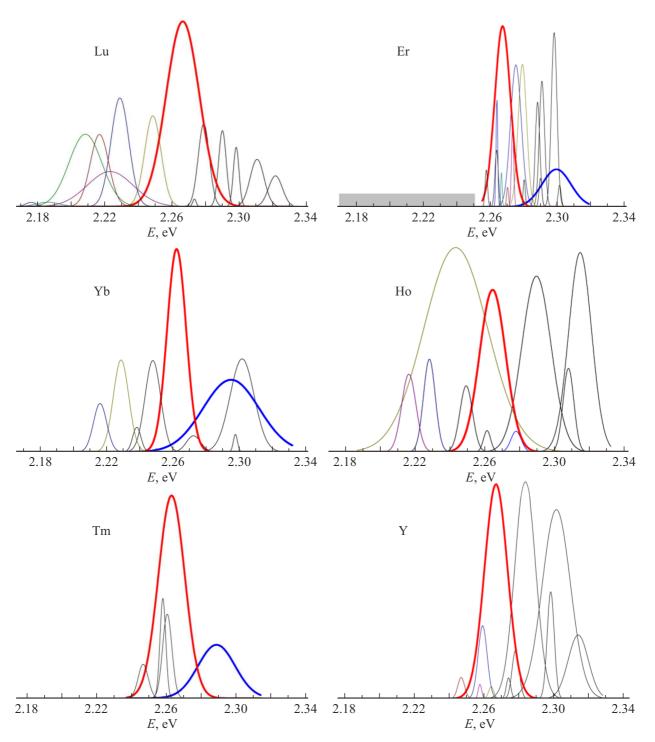
Figure 13. Detailed structure of the observed luminescence lines of bands in the area of $530-550$ nm for solid solutions based on hafnium dioxide. In the case of erbium, a area of the spectrum is marked where lines cannot be distinguished from -due to the dominance of cation luminescence bands. The energy of thermal excitation kT is of the order of 0.025 eV.

to note that completely similar bands were observed for zirconium dioxide doped with yttrium [30]. Moreover, bands with a wavelength of about 550 nm (2.25eV) were observed only when the crystal was irradiated by a source with a wavelength of 266 nm (4.66eV). When using a harder source (213 nm, 5.82 eV), luminescence was

observed at 460 nm (2.69 eV), and when using a softer (355 nm, 3.49 eV) — at 600 nm (2.07 eV).

To consider the details of the band structure, the results were rearranged depending on the quantum energy (Fig. 13 and 14). In the case of hafnium dioxide doped with lutetium, erbium and holmium, the bands are complicated
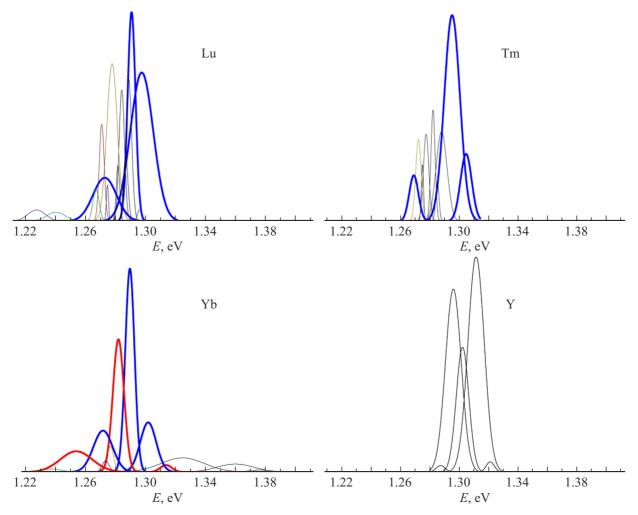
Figure 14. Detailed structure of the observed luminescence lines of bands in the area of 970 nm for solid solutions based on hafnium dioxide. In the case of ytterbium, the triplet of ytterbium proper is highlighted in red, which coincides with the one obtained in other matrices. Bands identical in the spectra of these samples are highlighted in blue.

by luminescence of the corresponding cations (Table 2). In turn, the spectra of ytterbium, thulium and yttrium reflect the properties of the defective structure of the material. We note the presence in all cases of a sufficiently intense one and the same band (highlighted in red in Fig. 13) with an energy of the order of 2.26 eV. It- seems that the same type of defects is a source of luminescence both in materials with a fluorite structure (both based on hafnium dioxide and zirconium dioxide) and in yttrium oxide. Obviously, this can only be a defect caused by an oxygen vacancy.

We note the weak lines (Fig. 13) for the sample doped with thulium. Luminescence in this area was observed for glasses [67,68] and referred to the thulium cation. According to the analysis of energy transitions in the thulium cation in different media [56–58], there should be no proper transitions of the cation with such energy. At the same time, the influence of the environment on the displacement of the energy f- levels [58] is actively discussed in the literature. The question of the nature of these lines requires additional research.

Fig. 14 shows the detailed structure of the observed luminescence lines of bands in the area of 970 nm; Fig. 6, d and Fig. 12 for a sample doped with ytterbium, there is a bright triplet due to the luminescence of this particular cation. This triplet is also highlighted in red in Fig. 14. Obviously, in addition to it, there is another strong triplet, which does not depend on the doping cation (Fig. 14), but is absent for materials based on zirconium dioxide [35]. The analysis carried out on the possibility of these lines belonging to some-or impurity cation did not yield results, since impurities in the amount of at least 100 ppm, considered as the cause of their occurrence, were not detected. Thus, this triplet, as well as the band near 690 nm (Fig. 2), reflect the properties of the defective structure of solid solutions based on hafnium dioxide.

We note that in addition to it, additional bands are observed for samples doped with thulium and lutetium (Fig. 14), which gives us reason to indicate in the table 2 the presence of intrinsic luminescence for these cations.

In this paper, we began to obtain splitting and displacement of luminescence lines caused by transitions between f-levels under the action of the surrounding REM-cation field. This is a promising tool for tracking the symmetry of the first coordination sphere. Such works on the example of the ytterbium cation already exist [71] and will be one of the subjects of further research.

5. Conclusion

Using Raman spectrometers of different wavelengths, solid solutions based on hafnium dioxide doped with six different cations were studied: Lu, Yb, Tm, Er, Ho, Y. Stokes lines independent of the wavelength of the laser used are highlighted. The dependence of the spectral lines of Raman scattering of light on the ratio of the radii of the doping and base cations is shown.

All non-Stokes lines are due to luminescence. The results obtained on Raman spectrometers, depending on the wave numbers, are rearranged in wavelength coordinates, which made it possible to compare them with the literature data on luminescence. In addition to luminescence caused by the participation of f-levels of REM cations, luminescence lines of the actual matrix of the material are observed. This effect is observed for the first time for materials based on hafnium dioxide, although similar effects are already known for solid solutions based on zirconium dioxide.

Conflict of interest

The authors declare that they have no conflict of interest.

References

[1] V.N. Chebotin, M.V. Perfilyev. Elektrokhimiya tverdykh elektrolitov. Khimiya, M. (1978). 312 p. (in Russian).

[2] M.V. Perfilyev, A.K. Demin, B.L. Kuzin, A.S. Lipilin. Vysokotemperaturny elektroliz gazov. / Edited by S.V. Karpachev. Nauka, M. (1988). 232 p. (in Russian).

[3] V.N. Chebotin. Khimicheskaya diffuziya v tverdykh telakh. Nauka, M. (1989). 208 p. (in Russian).

[4] H.L. Tuller, M. Balkanski, T. Takahashi. Solid State Ionics. Elsevier, Amsterdam (1992). 345 p.

[5] A.K. Ivanov-Shitz, I.L. Murin. Ionika tverdogo tela. SPbSU, SPb (2000). T. 1. 617 p. (in Russian).

[6] S.C. Singhal, K. Kendall. High Temperature Solid Oxide Fuel Cells: Fundamentals, Design and Applications. Elsevier, Amsterdam (2003). 429 p.

[7] J. Maier. Physical Chemistry of Ionic Materials: Ions and Electrons in Solids. Wiley, N.Y. (2004). 539 p.

[8] A.K. Ivanov-Shitz, I.L. Murin. Ionika tverdogo tela. SPbSU, SPb (2000). T. 2. 1000 p. (in Russian).

[9] F. Ramadhani, M.A. Hussain, H. Mokhlis, S. Hajimolana. Renew. Sustain. Energy Rev. 76, (2017). P. 460. DOI: 10.1016/j.rser.2017.03.052

[10] T. Liu, X. Zhang, X. Wang, J. Yu, L. Li. Ionics 22, 12, 2249 (2016). DOI: 10.1007/s11581-016-1880-1

[11] S.N. Shkerin. Izv. AN. Ser. fiz. 66, 6, 890 (2002) (in Russian).

[12] S. Shkerin. The YSZ Electrolyte Surface Layer: Existence, Properties and Effect on Electrode Characteristics. In: N.M. Sammes, A. Smirnova, O. Vasylyev. Fuel Cell Technologies: State and Perspectives. Springer, Dordrecht (2005). P. 301−306. DOI: 10.1007/1-4020-3498-9_34

[13] V. Ivanov, S. Shkerin, A. Rempel, V. Khrustov, A. Lipilin, A. Nikonov. J. Nanosci. Nanotechnol. 10, 11, 7411 (2010). DOI: 10.1166/jnn.2010.2836

[14] V. Ivanov, S. Shkerin, A. Rempel, V. Khrustov, A. Lipilin, A. Nikonov. Dokl. RAN 433, 2, 206 (2010). (in Russian).

[15] A.N. Vlasov. Elektrokhimiya 25, 5, 699 (1989) (in Russian).

[16] A.N. Vlasov. Elektrokhimiya 25, 10, 1313 (1989) (in Russian).

[17] A.N. Vlasov, I.G. Shulik. Elektrokhimiya 26, 7, 909 (1990). (in Russian).

[18] A.N. Vlasov. Elektrokhimiya 19, 2, 1624 (1983).

[19] A.N. Vlasov, M.V. Inozemtsev. Elektrokhimiya 21, 6, 764 (1985).

[20] A.N. Vlasov, M.V. Perfiliev. Solid State Ionics 25, 4, 245 (1987).

[21] A.N. Vlasov. Elektrokhimiya 27, 11, 1479 (1991).

[22] M.A. Borik, A.V. Kulebyakin, I.E. Kuritsyna, E.E. Lomonova, V.A. Myzina, P.A. Popov, F.O. Milovich, N.Yu. Tabachkova. FTT 61, 12, 2390 (2019). (in Russian). DOI: 10.21883/FTT.2019.12.48560.08ks

[23] D.A. Agarkov, M.A. Borik, G.M. Korableva, A.V. Kulebyakin, I.E. Kuritsyna, E.E. Lomonova, F.O. Milovich, V.A. Myzina, P.A. Popov, P.A. Ryabochkina, N.Y. Tabachkova. FTT 62, 12, 2093 (2020) (in Russian). DOI: 10.21883/FTT.2020.12.50213.160, translated version: 10.1134/S1063783420120021

[24] Z. Wang, Z.Q. Chen, J. Zhu, S.J. Wang, X. Guo. Radiation Phys. Chem. 58, 5−6, 697 (2000). DOI: 10.1016/S0969-806X(00)00242-5

[25] V.G. Keramidas, W.B. White. J. Chem. Phys. 59, 3, 1561 (1973). DOI: 10.1063/1.1680227

[26] E.E. Lomonova, D.A. Agarkov, M.A. Borik, G.M. Yeliseeva, A.V. Kulebyakin, I.E. Kuritsyna, F.O. Milovich, V.A. Myzina, V.V. Osiko, A.S. Chislov, N.Yu. Tabachkova. Elektrokhimiya 56, 2, 127 (2020). (in Russian). DOI: 10.31857/S0424857020020085

[27] D.A. Long. The Raman effect: A Unified Treatment of the Theory of Raman Scattering by Molecules. John Wiley & Sons Ltd, New Jersey (2002). 597 p. DOI: 10.1002/jrs.987

[28] S.N. Shkerin, E.S. Yulyanova, E.G. Vovkotrub. Neorgan. materialy 57, 11, 1213 (2021). DOI: 10.31857/S0002337X21100134

[29] S.H. Batygov, V.I. Vashchenko, S.V. Kudryavtsev, I.M. Klimkovich, E.E. Lomonova. FTT **30**, *3*, 661 (1988). (in Russian).

[30] N.G. Petrik, D.P. Taylor, T.M. Orlando. J. Appl. Phys. **85**, *9*, 6770 (1999). DOI: 10.1063/1.370192

[31] J.-M. Costantini, F. Beuneu, M. Fasoli, A. Galli, A. Vedda, M. Martini. J. Phys.: Condens. Matter. **23**, *11*, 115901 (2011). DOI: 10.1088/0953-8984/23/11/115901

[32] W.S.C. de Sousa, D.M.A. Melo, J.E.C. da Silva, R.S. Nasar, M.C. Nasar, J.A. Varela. Cerâmica **53**, 325, 99 (2007). DOI: 10.1590/S0366-69132007000100015

[33] K. Smits, L. Grigorjeva, D. Millers, A. Sarakovskis, J. Grabis, W. Lojkowski. J. Luminescence **131**, *10*, 2058 (2011). DOI: 10.1016/j.jlumin.2011.05.018

[34] L. Dunyushkina, A. Pavlovich, A. Khaliullina. Mater. **14**, *18*, 5463 (2021). DOI: 10.3390/ma14185463

[35] S.N. Shkerin, E.S. Yulyanova, E.G. Vovkotrub. FTT **64**, *4*, 467 (2022). DOI: 10.21883/FTT.2022.04.52187.252

[36] S. Stepanov, O. Khasanov, E. Dvilis, V. Paygin, D. Valiev, M. Ferrari. Ceram. Int. **47**, *5*, 6608 (2021). DOI: 10.1016/j.ceramint.2020.10.250

[37] R. Khabibrakhmanov, A. Shurukhina, A. Rudakova, D. Barinov, V. Ryabchuk, A. Emeline, G. Kataeva, N. Serpone. Chem. Phys. Lett. **742**, 137136 (2020). DOI: 10.1016/j.cplett.2020.137136

[38] N.C. Horti, M.D. Kamatagi, S.K. Nataraj, M.S. Sannaikar, S.R. Inamdar. AIP Conf. Proceed. **2274**, *1*, 020002 (2020). DOI: 10.1063/5.0022460

[39] X. Tan, S. Xu, L. Zhang, F. Li, B.A. Goodma, W. Deng. Appl. Phys. A **124**, *12*, 853 (2018). DOI: 10.1007/s00339-018-2284-z

[40] K. Smits, D. Olsteins, A. Zolotarjovs, K. Laganovska, D. Millers, R. Ignatans, J. Grabis. Sci. Rep. **7**, 44453 (2017). DOI: 10.1038/srep44453

[41] K. Smits, L. Grigorjeva, D. Millers, K. Kundzins, R. Ignatans, J. Grabis, C. Monty. Opt. Mater. **37**, 251 (2014). DOI: 10.1016/j.optmat.2014.06.003

[42] K. Smits, D. Jankovic, A. Sarakovskis, D. Millers. Opt. Mater. **35**, *3*, 462 (2013). DOI: 10.1016/j.optmat.2012.09.038

[43] L.A. Diaz-Torres, O. Meza, D. Solis, P. Salas, E. De la Rosa. Opt. Lasers Eng. **49**, *6*, 703 (2011). DOI: 10.1016/j.optlaseng.2010.12.010

[44] K. Smits, L. Grigorjeva, D. Millers, A. Sarakovskis, A. Opalinska, J.D. Fidelus, W. Lojkowski. Opt. Mater. **32**, *8*, 827 (2010). DOI: 10.1016/j.optmat.2010.03.002

[45] K. Utt, S. Lange, M. Jarvekulg, H. Mandar, P. Kanarjov, I. Sildos. Opt. Mater. **32**, *8*, 823 (2010). DOI: 10.1016/j.optmat.2010.02.016

[46] L.A. Diaz-Torres, E. De la Rosa-Cruz, P. Salas, C. Angeles-Chavez. J. Phys. D **37**, *18*, 2489 (2004). DOI: 10.1088/0022-3727/37/18/004

[47] V.B. Glushakova, M.V. Kravchinskaya, A.K. Kuznetsov, P.A. Tikhonov. Dioksid gafniya i ego soedineniya s oksidami redkozemelnykh elementov. Nauka, L. (1984). 174 p. (in Russian).

[48] S.V. Zhidovinova, A.G. Kotlyar, V.N. Strekalovsky, S.F. Palguev. Tr. In-ta of Electrochemistry of the UNC of the USSR Academy of Sciences **18**, 148 (1972).

[49] M.F. Trubelja, V.S. Stubican. Solid State Ionics **49**, 89 (1991).

[50] A.N. Meshcherskikh, A.A. Kolchugin, B.D. Antonov, L.A. Dunyushkina. FTT **62**, *1*, 145 (2020). (in Russian). DOI: 10.21883/FTT.2020.01.48752.557 [A.N. Meshcherskikh translated version: DOI:10.1134/S1063783420010229]

[51] S.N. Shkerin, M.V. Perfilyev. Elektrokhimiya **26**, *11*, 1461 (1990).

[52] M. Alotaibi, L. Li, A.R. West. Phys. Chem. Chem. Phys. **23**, *45*, 25951 (2021). DOI: 10.1039/d1cp04642j

[53] T. Ito, M. Maeda, K. Nakamura, H. Kato, Y. Ohki. J. Appl. Phys. **97**, *5*, 054104 (2005). DOI: 10.1063/1.1856220

[54] M. Villanueva-Ibaẽz, C. Le Luyer, C. Dujardin, J. Mugnier. Mater. Sci. Eng. **B105**, *1−3*, 12 (2003). DOI: 10.1016/j.mseb.2003.08.006

[55] L. Mariscal-Becerra, M.C. Flores-Jiménez, M. Hernández-Alcántara, E. Camarillo, C. Falcony-Guajardo, R. Vázquez-Arreguín, H. Murrieta Sanchez. J. Nanophotonics **12**, *3*, 036013 (2018). DOI: 10.1117/1.JNP.12.036013

[56] Yu.K. Voronko, B.I. Denker, V.V. Osiko. FTT **13**, *8*, 2193 (1971). (in Russian).

[57] W.T. Carnall, G.L. Goodman, K. Rajnak, R.S. Rana. J. Chem. Phys. **90**, *7*, 3443 (1989). DOI: 10.1063/1.455853

[58] J.C.G. Búnzli, C. Piguet. Chem. Soc. Rev. **34**, *12*, 1048 (2005). DOI: 10.1039/B406082M

[59] A. Ćirić, S. Stojadinović. J. Lumin. **26**, *17*, 116762 (2020). DOI: 10.1016/j.jlumin.2019.116762

[60] A. Konrad, U. Herr, R. Tidecks, F. Kummer, K. Samwer. J. Appl. Phys. **90**, *7*, 3516 (2001). DOI: 10.1063/1.1388022

[61] O. Kalantaryan, V.N. Karazin, V. Zhurenko, S. Kononenko, R. Skiba, V. Chishkala, M. Azarenkov. 2020 IEEE 10th Int. Conf. Nanomater.: Applications & Properties (NAP) P. 01NP03 (2020). DOI: 10.1109/NAP51477.2020

[62] V.I. Solomonov, V.V. Osipov, V.A. Shitov, K.E. Lukyashin, A.S. Bubnova. Optika i spektroskopiya **128**, *1*, 5 (2020). (in Russian). DOI: 10.21883/OS.2020.01.48831.117-19

[63] L. Li, X. Zhang, X. Wei, G. Wang, C. Guo. J. Nanosci. Nanotechnol. **14**, *6*, 4313 (2014). DOI: 10.1166/jnn.2014.8049

[64] L.Q. An, J. Zhang, M. Liu, S.W. Wang. Key Eng. Mater. **280−283**, *28*, 521 (2005). DOI: 10.4028/www.scientific.net/KEM.280-283.521

[65] N.A. Safronova, R.P. Yavetskiy, O.S. Kryzhanovska, S.V. Parkhomenko, A.G. Doroshenko, M.V. Dobrotvorska, A.V. Tolmachev, R. Boulesteix, A. Maitre, T. Zorenko, Yu. Zorenko. Opt. Mater. **101**, 109730 (2020). DOI: 10.1016/j.optmat.2020.109730

[66] Y. Yu, Y. Huang, L. Zhang, Z. Lin, G. Wang. PLoS ONE **8**, *1*, e54450 (2013). DOI: 10.1371/journal.pone.0054450

[67] S. Nishimura, S. Fuchi, Y. Takeda. J. Mater. Sci.: Mater. Electron. **26**, *8*, 10, 7157 (2017). DOI: 10.1007/s10854-017-6699-7

[68] S. Nishimura, Y. Nanai, S. Koh, S. Fuchi. J. Mater. Sci: Mater. Electron. **32**, *11*, 14813 (2021). DOI: 10.1007/s10854-021-06035-w

[69] K. Bhargavi, M.S. Rao, N. Veeraiah, B. Sanyal, Y. Gandhi, G.S. Baskaran. Int. J. Appl. Glass Sci. **6**, *2*, 128 (2014). DOI: 10.1111/ijag.12100

[70] X. Tan, S. Xu, L. Zhang, F. Liu, B.A. Goodman, W. Deng. Appl. Phys. A **124**, *12*, 853 (2018). DOI: 10.1007/s00339-018-2284-z

[71] T. Kallel, M.A. Hassairi, M. Dammak, A. Lyberis, P. Gredin, M. Mortier. J. Alloys. Compounds **584**, 261 (2014). DOI: 10.1016/j.jallcom.2013.09.057